

Original Article

# Applying Geophysical Methods for Site Characterization: A Case Study in Selangor, Malaysia

Iman Farshchi<sup>1</sup>, Mohamad Syazwan Bin Shaharudin<sup>2</sup>, Mohamad Zulhairi bin Mohd Bosro<sup>3</sup>

<sup>1,2,3</sup>Faculty of Engineering, Built Environment and IT, MAHSA University, Selangor, Malaysia.

<sup>1</sup>Corresponding Author : [iman.farshchi@gmail.com](mailto:iman.farshchi@gmail.com)

Received: 08 January 2025

Revised: 07 February 2025

Accepted: 05 March 2025

Published: 29 March 2025

**Abstract** - Subsurface conditions play a critical role in the structural integrity of foundations. Traditional drilling methods often offer limited insights, creating a need for complementary techniques that provide more comprehensive subsurface imaging at lower costs and greater efficiency. This study integrates geophysical methods—specifically Seismic Refraction and Electrical Resistivity Imaging (ERI)—to conduct a pre-foundation site assessment at MAHSA University in Bandar Saujana Putra, Malaysia. Geologically, the area is characterized by the Kenny Hill Formation, an Upper Paleozoic sedimentary sequence overlain by alluvial soils. Seismic Refraction was used to determine subsurface layering and material velocities, with geophones capturing refracted wave data to construct velocity and depth profiles. The ERI survey employed the Wenner and Schlumberger configuration to map resistivity variations, indicating soil composition and geological features. Interpretation of seismic and resistivity data revealed details on soil strength, weathering profiles, and rippability, enhancing site suitability assessment. The analysis identified three main material layers. The first layer, classified as Weathering Grade VI, consists of completely weathered material decomposed into soil, reaching a depth of about 6–9 meters. With a Weathering Grade V classification, the second layer is also considered rippable and extends beyond 15 meters in depth. Finally, denser material was found below 15 meters, classified as Weathering Grade IV; this layer is moderately weathered, still rippable, but approaching a marginal level. Results highlight the value of integrating geophysical methods in foundation engineering, offering improved reliability over conventional soil testing by delineating soil-rock interfaces and subsurface heterogeneities critical for foundation stability.

**Keywords** - Geophysical survey, Geotechnical site investigation, Seismic refraction, Electrical Resistivity Imaging (ERI), Bandar saujana putra, Selangor.

## 1. Introduction

Extensive research has consistently highlighted that ground conditions represent the most significant technical and financial risks in civil engineering projects [1-3]. Structural foundation failures are often traced back to insufficient or improper geotechnical investigations. When site assessments are inadequate, engineers must compensate by overdesigning foundations to mitigate failure risks, substantially raising project costs.

Numerous studies have reported cases where inadequate site investigations in highly variable soil conditions led to foundation failures, resulting in major cost overruns and project delays [3-5]. An analysis of 89 underground projects in the United States revealed that over 85% had insufficient geotechnical investigations, failing to adequately assess site conditions and leading to claims and budget overruns [1]. Similarly, the National Economic Development Office (NEDO) examined 56 industrial building projects and found that nearly half experienced at least one-month delays, with

37% encountering setbacks due to ground-related challenges such as water and rock conditions [6]. Therefore, selecting a precise and suitable site investigation method is essential for achieving safe, efficient, cost-effective foundation designs.

Conventional drilling methods provide limited point-based data on subsurface conditions, which may not always capture the full complexity of soil heterogeneity and potential geohazards. This limitation often leads to uncertainties in foundation design, increasing the risk of structural instability and unforeseen construction challenges.

While geophysical techniques have been increasingly used to complement traditional site investigations, there remains a gap in systematic integration and comparative analysis of different methods to enhance site characterization accuracy.

Numerous studies have demonstrated the benefits of incorporating geophysical approaches with standard soil



testing to mitigate risks associated with weak or unstable ground conditions. Geophysical techniques are widely applied across various disciplines, including construction site assessments and the inspection of dams and dikes. These methods facilitate the analysis of geological formations and the evaluation of key physical properties of rock structures [7-12].

Geophysics, as a field of study, examines the Earth's physical characteristics-such as electrical resistivity, velocity, density, magnetic field, and magnetic susceptibility-using principles of physics. In practical applications, geophysics serves as an interdisciplinary domain where physics-based methodologies are employed to investigate subsurface conditions [13].

One of the primary advantages of geophysical methods is their ability to accurately and efficiently detect underground features without requiring invasive procedures such as drilling or boreholes [14]. In recent decades, these techniques have become essential for soil characterization. However, ongoing discussions persist regarding their accuracy and the interpretation of results [15].

Geophysical investigations provide the distinct benefit of offering a broad and detailed subsurface perspective while enabling rapid and cost-effective data acquisition [16]. These methods facilitate the collection of precise and reliable information on underground conditions [17]. However, the effectiveness of electrical resistivity techniques is subject to physical constraints, including resolution, penetration depth, and signal-to-noise ratio, which may influence data quality and reliability [18].

Selecting an appropriate geophysical method depends on several key factors. First, the study's objectives must be clearly defined, whether they pertain to groundwater detection, rock characterization, soil analysis, or the identification of subsurface cavities and archaeological sites. Second, the choice of technique should correspond to the specific physical properties being measured, as different parameters require specialized methods. Third, the selected methodology and its configuration should be tailored to align with the study's requirements. Additionally, environmental conditions, such as site noise levels, must be considered, as they can impact data accuracy. Finally, reviewing existing literature or previously published data relevant to the study area can enhance the reliability and validity of the analysis [19].

Although Numerous studies have demonstrated the benefits of incorporating geophysical approaches, there is still a need for practical case studies that validate the effectiveness of these methods in real-world construction settings, particularly in rapidly developing regions where

urban expansion demands reliable and cost-efficient ground investigation solutions.

This research addresses this gap by conducting a pre-foundation site characterization using Seismic Refraction and Electrical Resistivity Imaging (ERI) at a project site at MAHSA University in Bandar Saujana Putra, Jenjarom, Selangor, Malaysia. This study aimed to highlight the value of engineering geophysics in subsurface investigations by comparing the results of these two techniques, ultimately providing a comprehensive assessment of soil conditions to support foundation design decisions.

A distinguishing aspect of this research is its focus on both the selected study area and the comparative evaluation of Seismic Refraction and Electrical Resistivity Imaging (ERI) for site characterization. While many studies have utilized geophysical techniques, limited research has focused on evaluating these methods in developing urban areas where precise foundation assessments are critical.

By systematically comparing the strengths and limitations of Seismic Refraction and ERI, this study enhances the understanding of their complementary roles in subsurface investigations. The findings contribute to improved decision-making in foundation design and provide a valuable reference for integrating multiple geophysical methods in similar geotechnical studies.

## 2. Project Description

The project area is located at Bandar Saujana Putra, Jenjarom, Selangor, Malaysia, at approximately 2°57'37.0 "N 101°34'34.0" E. The survey line position was determined based on suitable and available areas. One (1) Line of seismic refraction and one (1) electrical resistivity imaging was done.

This region is largely unexplored but is underlain by alluvium atop the Kenny Hill Formation. Granite plutons have intruded into all bedrock layers. The Kenny Hill Formation is a metamorphosed clastic sedimentary sequence [20, 21] formed during the Upper Silurian to Devonian periods. It appears as a broad synclinal belt featuring a consistent sequence of Upper Paleozoic interbedded shales, mudstones, siltstones, and sandstones. The subsurface examination indicates that, along this route, the Kenny Hill Formation is composed of alternating layers of sandstones, siltstones, and shales/mudstones, topped by dense, over-consolidated soils mainly made up of sandy-silty clay and silty sand. Across the region, the level of metamorphism within the Kenny Hill Formation differs, with certain areas experiencing low-grade metamorphism that altered sandstone into quartzite and shale into phyllite, while higher grades converted shales into schist. The geological data for the Bandar Saujana Putra location in Jenjarom, Selangor, is emphasized in the red box in Figure 1.

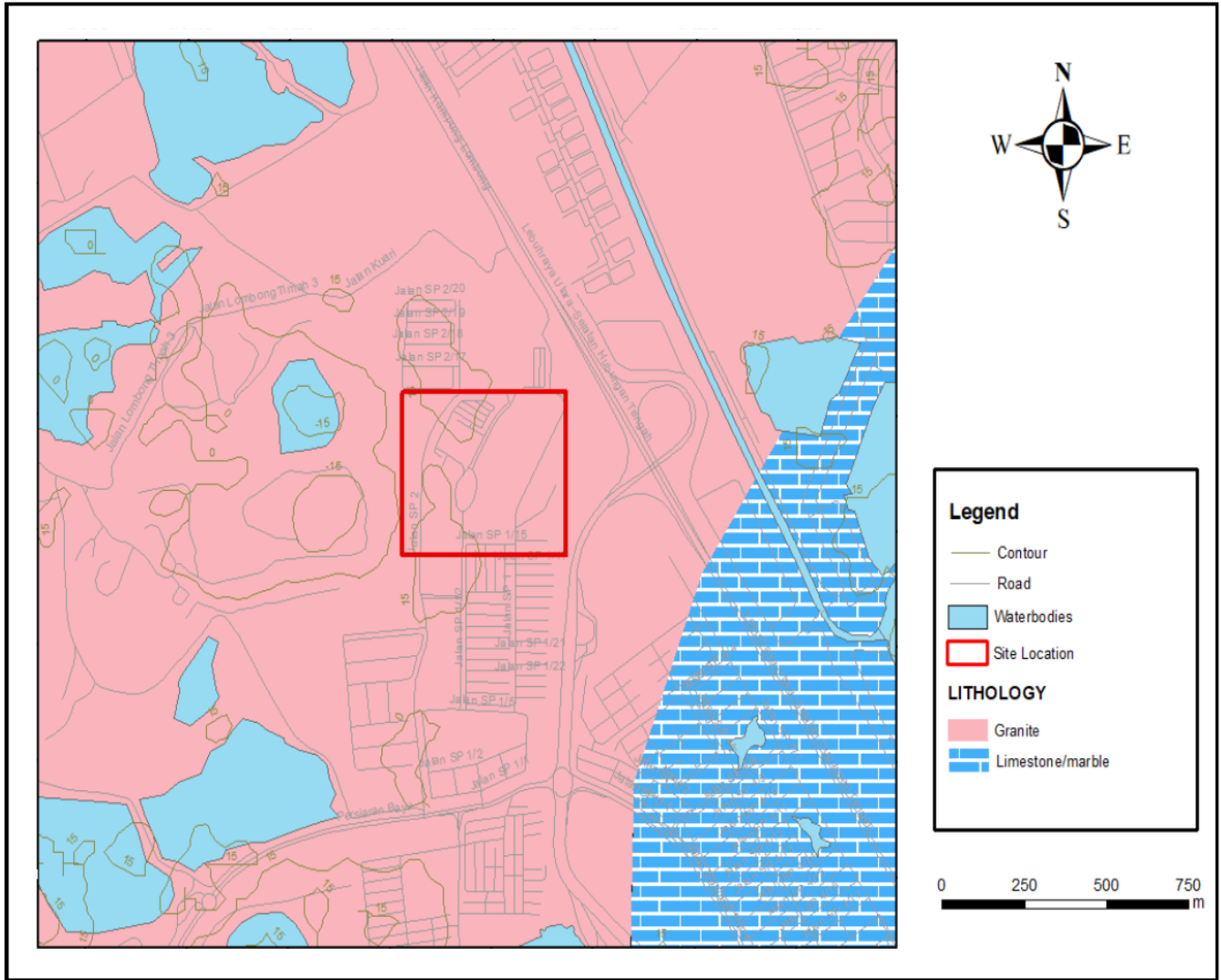


Fig. 1 General geology map at Bandar Saujana Putra, Jenjarom, Selangor (Department of Mineral and Geoscience Malaysia (JMG))

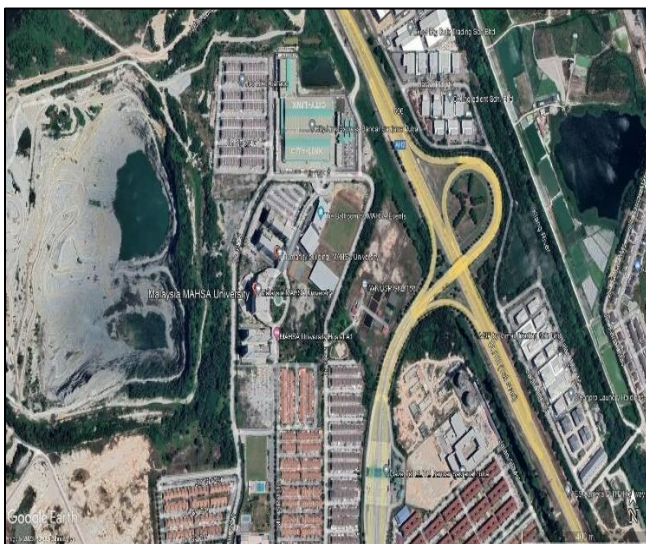


Fig. 2 Location of site at Bandar Saujana Putra, Jenjarom, Selangor



Fig. 3 Location of site at Bandar Saujana Putra, Jenjarom, Selangor

### 3. Methodology

#### 3.1. 2D Seismic Refraction

##### 3.1.1. Introduction to Seismic Refraction Method

Seismic refraction tomography, also referred to as velocity gradient or diving-wave tomography, utilizes the first-arrival time of seismic waves as its primary data input [22, 23]. In contrast to traditional refraction methods that rely on distinct velocity contrasts between layers, this approach treats the subsurface as a continuous medium, allowing for a more refined depiction of velocity variations with depth. By modeling the velocity gradient, it provides valuable insights into geological formations.

This technique employs generalized simulated annealing, an optimization algorithm that iteratively performs forward modeling. Models are either accepted or rejected based on probabilistic criteria, enabling the algorithm to bypass local minima and achieve a globally optimized solution for the subsurface velocity structure. This process minimizes the risk of non-unique solutions, enhancing both accuracy and reliability. Furthermore, the algorithm does not impose constraints on the orientation of the velocity gradient, making it capable of detecting vertical structures and significant lateral velocity variations when present.

Seismic refraction tomography is particularly effective in regions with pronounced lateral velocity gradients, irregular topography, or complex near-surface conditions where prior knowledge of the subsurface structure is minimal [24].

Seismic techniques are widely applied for shallow-depth investigations and are frequently used to identify potential groundwater zones and analyze subsurface profiles in numerous locations today [25-27].

This approach involves tracking the travel time of an elastic wave, generated here by striking a steel plate with a hammer or alternatively by using a gun. The wave refracts upon reaching a subsurface layer and is then captured by geophones positioned on the surface.

##### 3.1.2. Stages of Seismic Refraction Method Energy Generation and Wave Propagation

The seismic refraction method begins with generating seismic energy using a surface source, or “shot.” Common sources for shallow applications include a hammer and plate, a weight drop, or a small explosive charge like a blank shotgun cartridge.

The energy radiates outward from the shot point, traveling either directly through the uppermost layer (direct arrivals) or downward to higher-velocity layers, where it travels laterally along these layers before returning to the surface (refracted arrivals). A linear array of geophones, spaced at regular intervals, detects this energy at the surface.

##### *Data Acquisition and Crossover Distance*

As seismic waves propagate, they are recorded at different geophones, with the refracted wave becoming the first-arrival signal at distances beyond the crossover distance. This crossover distance is the point at which refracted arrivals overtake direct arrivals in travel time.

Shots are placed at and beyond both ends of the geophone spread to ensure comprehensive data collection. These recordings capture first-arrival times for both direct and refracted signals, which are then stored on a seismograph and transferred to a computer for detailed analysis.

##### *Travel Time Analysis and Velocity Calculations*

Travel time data from each shot position is plotted against distance to generate travel time graphs. Gradients from the direct arrival and T-minus graphs are analyzed to determine the velocities of the overburden and refractor layers. These calculated velocities are crucial for interpreting subsurface materials' elastic and density properties. The processed graphs form the foundation for constructing depth profiles and velocity models.

##### *Depth Profiling and Visualization*

Using the measured travel times, calculated velocities, and shot-receiver geometry, depth profiles for refractor layers are generated. The final processed data is represented through time-distance graphs, true depth, and velocity profiles. Shot records, displayed as wiggle traces, facilitate an initial velocity estimation and serve as quality checks. Refractor depths are visualized as overlapping arcs beneath the intersections of neighboring arcs, refining the understanding of the subsurface layers' structure and depth.

##### *Applications and Validation*

This method has versatile applications, including determining the depth of bedrock, mapping bedrock structures, assessing rock quality, and evaluating the thickness of overburden. Examples include mapping the depth to the base of backfilled quarries and landfill thicknesses.

To validate results, ground truth data, such as borehole logs and trial pit records, is superimposed on depth profiles to confirm the correlation of seismic results along the survey line. This validation enhances the accuracy and reliability of the interpretations.

In the data acquisition phase, individual shot records are shown as variable area wiggle traces, depicting travel time versus distance (Figure 4). These displays enable an initial estimation of overburden and refractor apparent velocities while also serving as a quality check for the collected data. After the acquisition, wiggle traces are utilized to present the data during the selection of first arrivals for each geophone position and shot.

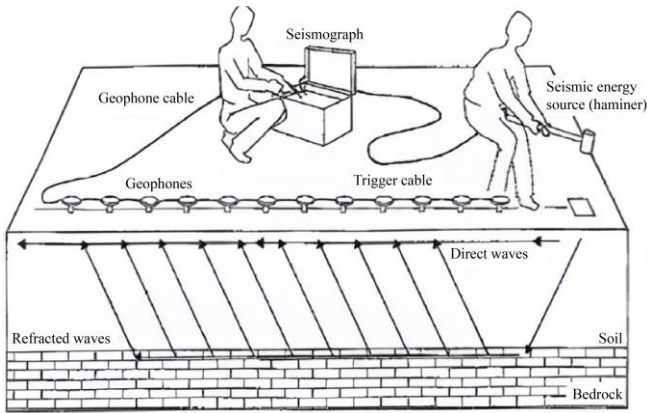


Fig. 4 Seismic refraction method (modified from ASTM D5777, 2006)

The processed information is typically presented in three distinct plots: time-distance graphs for the picked first arrivals on each shot, a true depth profile for the identified refractors, and a velocity profile for the overburden and refractors. Existing ground truth data, such as borehole and trial pit logs, is superimposed on the depth profile to assist in calibrating the seismic results and provide an indication of correlation along the survey line. The refractor depth is illustrated as a series of overlapping arcs, representing solutions for each geophone in the array. The refractor can be positioned anywhere on the arcs below the intersections with adjacent arcs.

Figure 5 illustrates the geophone arrangement and shot points along a seismic spread. Each spread consists of 24 geophones placed at 5m intervals and 9 shot points per spread, measured at -10.0 m, 0.0 m, 17.5 m, 37.5 m, 57.5 m, 77.5 m, 77.5 m, 97.5m, 115m, and 125 m along the ground surfaces.

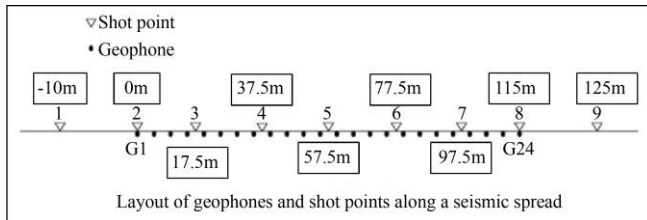


Fig. 5 Position of 9 shot points along the survey line Survey

### 3.1.3. Survey Steps

The survey commences by adhering to the sampling pattern outlined in the work plan, which involves locating, marking, and clearing survey lines before deploying seismic cables and positioning geophones. Subsequently, the seismograph and computer are set up, and geophone responses are evaluated. Shot preparation involves using either an 8kg hammer or a 20kg weight drop, followed by monitoring ambient noise and conducting seismic shots along the survey segment. The integrity of the shot data is then examined, with shots repeated if necessary. Equipment is relocated to the next survey segment, and the process from

cable layout to data inspection is repeated. Finally, the seismic data undergoes processing and interpretation to generate profiles and compile the survey report. The survey steps can be summarized as follows:

- Follow the sampling pattern outlined in the work plan.
- Locate, mark and clear survey lines.
- Layout seismic cables and set geophones.
- Set up seismograph and computer and test geophone responses.
- Prepare for the shot using a hammer (8kg) / weight drop (20kg).
- Monitor ambient noise and conduct seismic shots along the survey segment.
- Inspect the integrity of shot data - repeat if necessary.
- Move equipment to the next survey segment and repeat steps 3-7 above.
- Process and interpret seismic data.
- Prepare profiles and reports.

### 3.2. Equipment (Seismograph)

The seismograph used in this study was carried out using ABEM Seismograph. This system is connected to 24 geophones laid out on a straight.

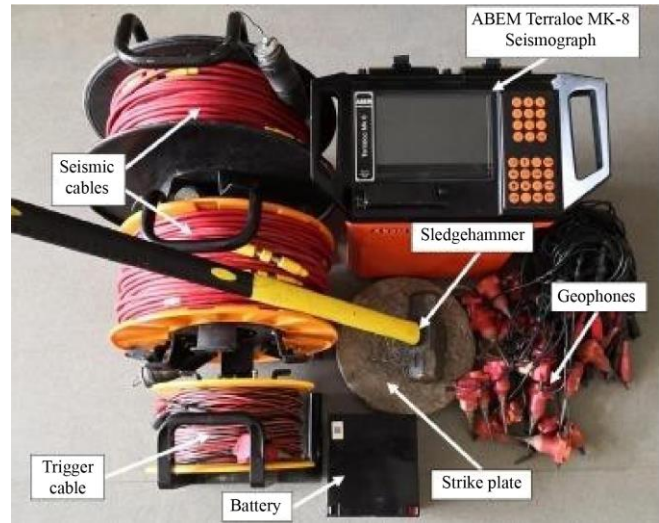


Fig. 6 Typical ABEM seismograph used for seismic refraction

## 4. Electrical Resistivity Imaging - ERI survey

Electrical Resistivity Imaging (ERI) is highly regarded for its non-invasive nature, cost efficiency, and effectiveness in subsurface investigations.

This method utilizes high-voltage alternating current with low amperage and low-power frequency to penetrate the ground, generating a detailed model of subsurface conditions. Specifically, in combination with induced polarization (IP) imaging, ERI maps the spatial distribution of resistive and capacitive properties of underground materials at low frequencies [28].

Resistivity refers to the ability of a specific material of a certain size to resist electrical conduction. While all materials oppose the flow of electrical current to some extent, some are more effective conductors than others. To give context to resistivity values, Ohms are used as the standard unit for a given material size.

Materials that readily conduct electrical current are classified as conductors and exhibit low resistivity, whereas those that do not easily conduct electricity are known as insulators and possess high resistivity. In the fields of geophysics and geotechnics, the terms “electrical resistivity” and “D.C. resistivity” are often used interchangeably. Various geological factors, such as clay content and soil or formation type, influence earth resistivity (and its inverse, conductivity).

Apparent resistivity is a measure that reflects the resistivity of an idealized, electrically uniform, and isotropic half-space, which produces the observed relationship between applied current and potential difference for a given electrode arrangement and spacing. This concept is derived by analyzing the potential distribution created by a single current electrode and formulating an equation that connects apparent resistivity with the applied current, potential, and electrode configuration.

The behavior of electrode pairs or other configurations can be understood through the principle of superposition. For instance, if a single point electrode is placed on the surface of a semi-infinite, electrically uniform medium representing a homogeneous earth, the potential at any point in or on the medium is determined by the current  $I$  flowing through the electrode. This relationship is mathematically expressed in an equation describing the potential distribution:

$$U = \rho \frac{1}{\pi r} \tag{1}$$

Where:

- $U$  = potential, in V,
- $\rho$  = resistivity of the medium,
- $r$  = distance from the electrode.

The mathematical demonstration for the derivation of the equation may be found in textbooks on geophysics, such as Keller and Frischknecht (1966) [29]. The selection of an array for conducting a field survey is influenced by the structure type to be mapped, the resistivity meter’s sensitivity, and the level of background noise. For 2-D imaging surveys, the most frequently employed arrays include (a) Wenner, (b) dipole-dipole, (c) Wenner-Schlumberger, (d) pole-pole, and (e) pole-dipole. Important characteristics to consider for an array are (i) its sensitivity to vertical and horizontal variations in subsurface resistivity, (ii) the depth it can investigate, (iii) the extent of horizontal data coverage, and (iv) the strength of the signal [30].

The Wenner-Schlumberger configuration features a constant spacing system characterized by the factor “ $n$ ,” which compares the distance between the electrodes C1-P1 (or C2-P2) with the distance between P1 and P2, as illustrated in Figure 7. When the distance between the potential electrodes (P1 and P2) is defined as “ $a$ ,” the distance between the current electrodes (C1 and C2) becomes  $2na + a$  [31]. This method for determining resistivity employs four electrodes arranged linearly. It combines elements of both the Wenner and Schlumberger configurations. When the spacing factor ( $n$ ) is set to 1, the Wenner-Schlumberger setup resembles the Wenner configuration, where the electrode distance is “ $a$ .” However, as  $n$  increases to 2 or more, the Wenner-Schlumberger configuration aligns more closely with the Schlumberger configuration, with the current electrodes positioned farther apart than the potential electrodes [31].

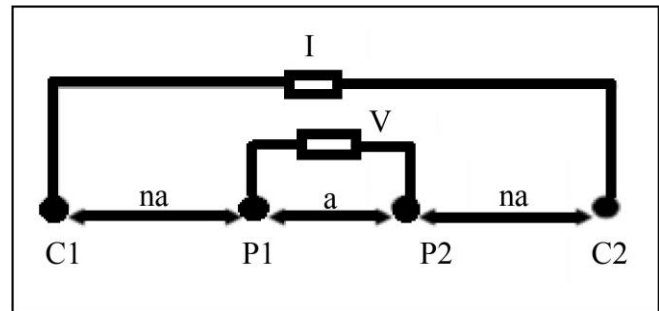


Fig. 7 The setting of Wenner - Schlumberger configuration electrode [31]

**4.1. Equipment (Electrical Resistivity Meter)**

The 2-D geo-electrical imaging survey in this study was carried out using ABEM SAS4000 resistivity meter and ABEM ES10-64 electrode selector or ABEM LS system. This system is connected to 41 electrodes for 200m, which were laid out on a straight line with 1.5-meter to 5-meter electrode spacing. The resistivity meter selects only four active electrodes used for each measurement. Figures 8 and 9 show the resistivity equipment used in this survey.



Fig. 8 Resistivity survey equipment – ABEM LS



Fig. 9 Resistivity survey equipment – ABEM SAS4000

## 5. Interpretation of Data

### 5.1. The Interpretation of Velocity and Rippability Scale for Seismic Refraction Survey

The seismic velocity of materials is influenced by characteristics of the soil or rock mass, including its hardness and strength, the degree of weathering, and the presence of discontinuities. The interpretation was based on the

weathering profile classification in Table 1 and the typical ranges of seismic velocity for weathering grade classification, as shown in Tables 2 and 3.

The boundary between rock and soil is determined by a velocity value of 1,400 m/s. If the velocity is below 1,400 m/s, it indicates soil or highly weathered rock. Conversely, a velocity above 1,400 m/s suggests difficult excavating rock.

For the rippability chart, a relationship was established between  $V_p$  and rock properties to enable general rippability assessments based on industry-standard charts and the geological characteristics of subsurface conditions. The chart in Figure 10 reflects the capacity of the smallest Caterpillar ripper, the D8R, to excavate material based on seismic compressional (P-wave) velocity, representing a conservative classification of rippability. Using available data and seismic survey results, localized correlations among velocity, material, weathering grade, and rippability were established (Tables 2 and 3). However, this correlation relies on current data and should be updated if new information becomes available.

Table 1. Classification of weathering profile [32]

Weathering Classification Term	Zone	Description
Residual Soil	VI	All rock material has transformed into soil, with the original mass structure and texture completely obliterated.
Completely Weathered	V	The rock material has fully decomposed into soil, though some material remains intact. It is sandy and becomes friable when soaked in water or squeezed by hand.
Highly Weathered	IV	The rock material is in a transitional phase towards becoming soil, existing as either soil or rock. It is entirely discolored, yet the fabric remains intact, with the mass structure partially preserved.
Moderately Weathered	III	The rock material exhibits partial discoloration, but the mass structure and texture are fully intact. Discontinuities are often filled with iron-rich material, and fragments or block corners can be chipped by hand.
Slightly Weathered	II	Discoloration occurs along discontinuities and may affect parts of the rock material. The mass structure and texture are fully preserved, though the material is generally weaker, and fragment corners cannot be chipped by hand.
Un-weathered	I	Most rock fragments retain their original shape.

Table 2. Weathering grade and the P-wave velocity [33]

Weathering Grade	P- Wave velocity (m/s)
I-II-III	>2400
II-III-IV	1800 - 2400
V-IV	800 - 1800
VI-V	300 - 800
VI	<300

Table 3. Correlation between velocity, material, weathering grade and rippability of soil/rocks

Velocity (m/s)	Material	Weathering Grade	Rippability
0 – 400	Soil	VI Residual Soil	Rippable
400 – 800	Soil	V Completely Weathered	Rippable
800 – 1200	Soil	IV Highly Weathered	Marginal
1200 – 1600	Rock	III Moderately	Marginal
1600 – 2000	Rock	II Slightly Weathered	Non - Rippable
2000 >	Rock	II-I Fresh Rock	Non - Rippable

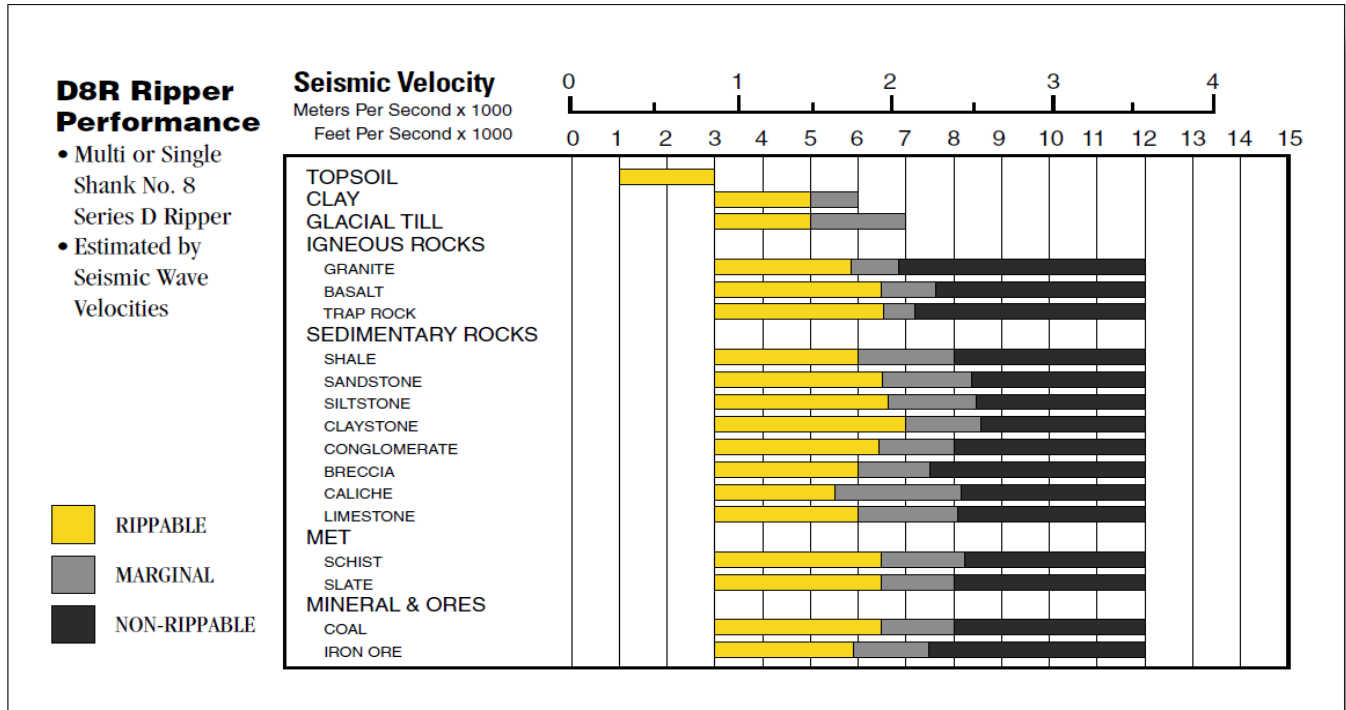


Fig. 10 Velocity, D8R Ripper performance chart based on seismic velocities [34]

**5.2. 2D Resistivity Analysis and Tomography for Electrical Resistivity Imaging - ERI Survey**

Resistivity geo-electrical surveys are conducted to outline the resistivity distribution in the subsurface, which arises due to the presence of various materials with distinct electrical properties. Figures 11 and 12 display resistivity ranges for different weathering conditions similar to those found in the studied area. A detailed examination of these ranges reveals differences spanning several orders of magnitude and overlapping values among classifications of weathering profiles and materials. This overlap reflects the complexity of subsurface conditions, where resistivity is influenced by multiple factors.

The electric current in shallow earth materials flows through two main mechanisms: electronic conduction and electrolytic conduction. Electronic conduction occurs via free electrons, as seen in metals, while electrolytic conduction results from ion movement in groundwater. In environmental and engineering surveys, electrolytic conduction is more common, whereas electronic conduction is significant in

mineral exploration, particularly when conductive minerals such as metal sulfides and graphite are present. The distinction between these mechanisms is crucial for interpreting resistivity data in different geological contexts.

Rigorous quality checks are performed during data collection, and any low-quality data is partially corrected. Specialized software is then used to invert the data and generate a soil resistivity model. This process results in the creation of resistivity tomography or pseudo-sections, as shown in the figures, representing fully processed resistivity data.

The final resistivity model provides a detailed representation of subsurface materials, considering factors such as the characteristics of the solid matrix, porosity, and the type of fluids occupying the pores, such as water or air.

The resistivity values of rocks and soils vary significantly, with dry materials typically exhibiting high resistivity values ranging from hundreds to thousands of ohm-meters. In contrast, fractured rock saturated with water

shows much lower resistivity values, generally below 1000 ohm-meters. Groundwater resistivity further depends on the concentration of electrolytes, with fresh groundwater usually having resistivity values between 10 and 100 ohm-meters. The variations in these values provide valuable insights into

the subsurface composition and fluid content. Resistivity ranges for various rocks, soil types, and chemicals have been documented in studies by Keller and Frischknecht (1966) and Telford et al. (1990) [27, 35].

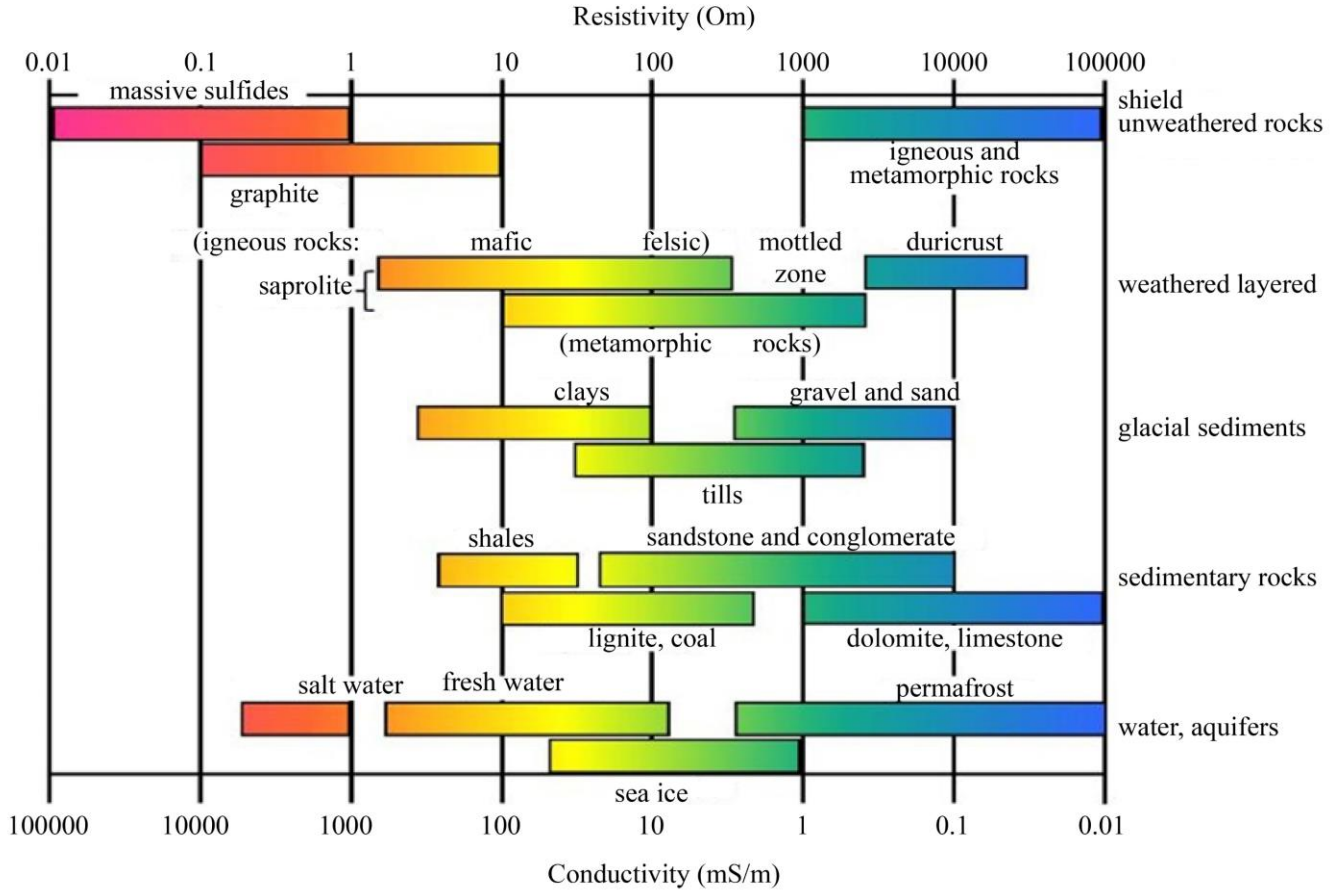


Fig. 11 Resistivity of soil or rock by Palacky 1987 [36]

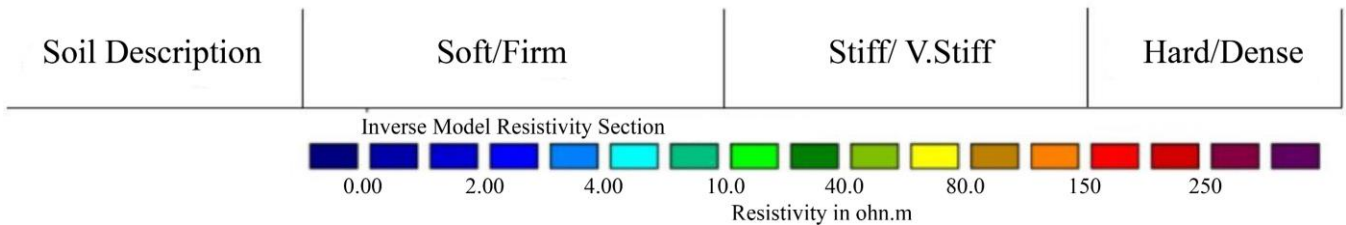


Fig. 12 Summary interpretation and correlation-based electrical resistivity

Igneous and metamorphic rocks, in particular, tend to exhibit high resistivity values, ranging from approximately 1000 to 10 million ohm-meters. These values depend heavily on the extent of fracturing and the presence of groundwater within fractures.

As a result, the same rock type can show a wide resistivity range depending on its moisture content. This variability is a critical factor in identifying fracture zones and other weathering features, making resistivity surveys

invaluable for engineering and groundwater investigations. The workflow for this method is outlined below:

### 5.2.1. Data Quality Checking

The process begins with thoroughly evaluating the acquired resistivity data to identify and remove erroneous or noisy measurements. This ensures that the dataset used for subsequent analysis is reliable and free from significant anomalies introduced by external factors such as instrumentation errors or environmental interference.

5.2.2. Topographical Correction

Given that surface terrain variations can influence resistivity measurements, topographical corrections are applied to account for elevation changes. This step adjusts the measured apparent resistivity values to reflect true subsurface conditions by incorporating elevation data into the inversion process.

5.2.3. Development of an Initial Model

An initial resistivity model is created based on the corrected data. This model serves as the starting point for inversion procedures, providing an estimated subsurface resistivity distribution that will be iteratively refined.

5.2.4. Prediction of Earth Model by Inversion

The inversion process begins by predicting an Earth model that best fits the observed resistivity measurements. The model is continuously updated to minimize discrepancies between measured and calculated resistivity values.

5.2.5. Input of Inversion Parameters

The inversion process requires specific parameters such as the number of iterations, damping factors, and convergence criteria. These parameters are inputted into the inversion algorithm to regulate the computation and refine the resistivity model.

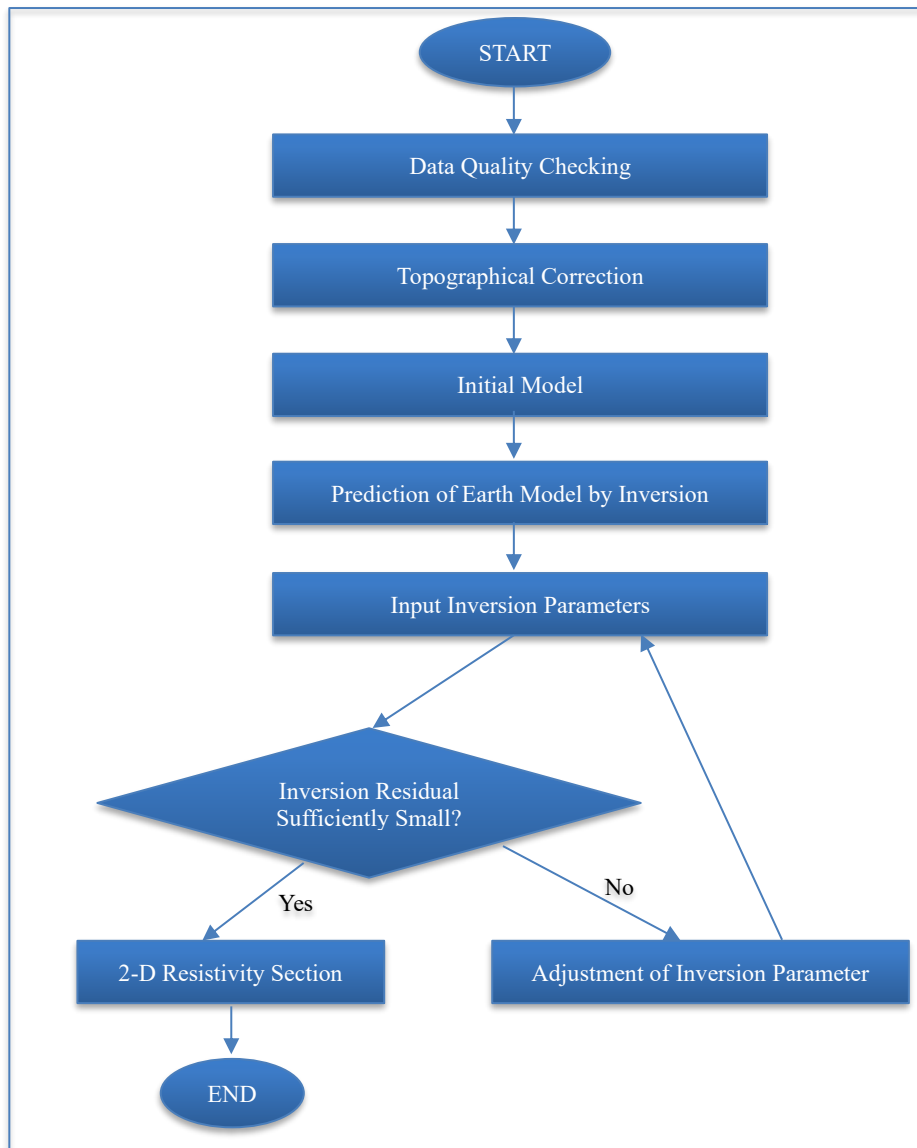


Fig. 13 Processing flowchart

5.2.6. Adjustment of Inversion Parameters

If the inversion results indicate significant residual errors, adjustments to the inversion parameters are made.

This iterative refinement ensures that the predicted model progressively aligns with observed field data.

5.2.7. Evaluation of Inversion Residual

A key criterion for determining the accuracy of the inversion process is the residual error, which represents the difference between observed and calculated resistivity values. The process proceeds to the final stage if the residual is sufficiently small. Otherwise, further adjustments to the inversion parameters are made, and the inversion process is repeated.

5.2.8. Generation of 2D Resistivity Section

Once the inversion residual falls within an acceptable threshold, the final 2D resistivity section is generated. This section provides a detailed representation of the subsurface resistivity distribution, aiding in geological and geotechnical interpretations. The described process ensures that the 2D resistivity imaging method effectively models subsurface conditions with high accuracy. Through iterative inversion adjustments and rigorous data validation, the method enhances the reliability of ERI surveys, making them valuable tools in geotechnical, hydrogeological, and environmental investigations (Figure 13).

6. Results and Discussion

This report summarizes findings from one (1) Seismic Refraction survey and one (1) Electrical Resistivity Imaging (ERI) lines conducted to assess subsurface conditions in a designated soil area. The objective was identifying layers, potential anomalies, and approximate bedrock depths.

6.1. Results of Seismic Refraction Survey

One (1) seismic line has been conducted to investigate subsurface information. The interpretation was based on typical ranges of seismic velocity for weathering grade classification, as shown in Tables 2 and 3, and the weathering

profile classification in Table 1. The Seismic Refraction survey provided velocity-based data to classify subsurface materials according to rippability and weathering grades. As shown in Figure 14, up to a recorded depth of 30 m, three main material categories have been detected. The first layer has a velocity range of 0–400 m/s, indicating soil with a Weathering Grade VI classification, which is considered rippable. This layer extends up to 5 m deep, reaching over 9 m in some areas.

The second layer has a velocity range of 400–800 m/s, representing Weathering Grade V soil, also classified as rippable, and extends from 5 m to over 15 m in depth. Finally, a velocity range of 800–1200 m/s is detected beyond 15 m depth, representing soils with a Weathering Grade IV classification, still rippable but approaching a marginal level. Bedrock was not detected within this depth range, indicating it may be located at a greater depth.

6.2 Results of Electrical Resistivity Imaging (ERI) Survey

6.2.1 Results of ERI Line (PROTOCOL SCHLUMBERGER)

Figure 15 shows the ERI survey results using the Schlumberger protocol, revealing a top layer suspected to be potential fill material extending to a depth of approximately 6-9 meters. This layer is thought to consist of uncompacted soil, indicating loose or disturbed fill with a value of up to 80 ohms.

Beneath this, a significant anomaly suggests a dense or hard layer, likely composed of compacted soil or possibly the original ground layer with a value of up to 220 ohms. Bedrock does not appear prominently in the profile, suggesting it is located deeper than the detectable range of this ERI survey.

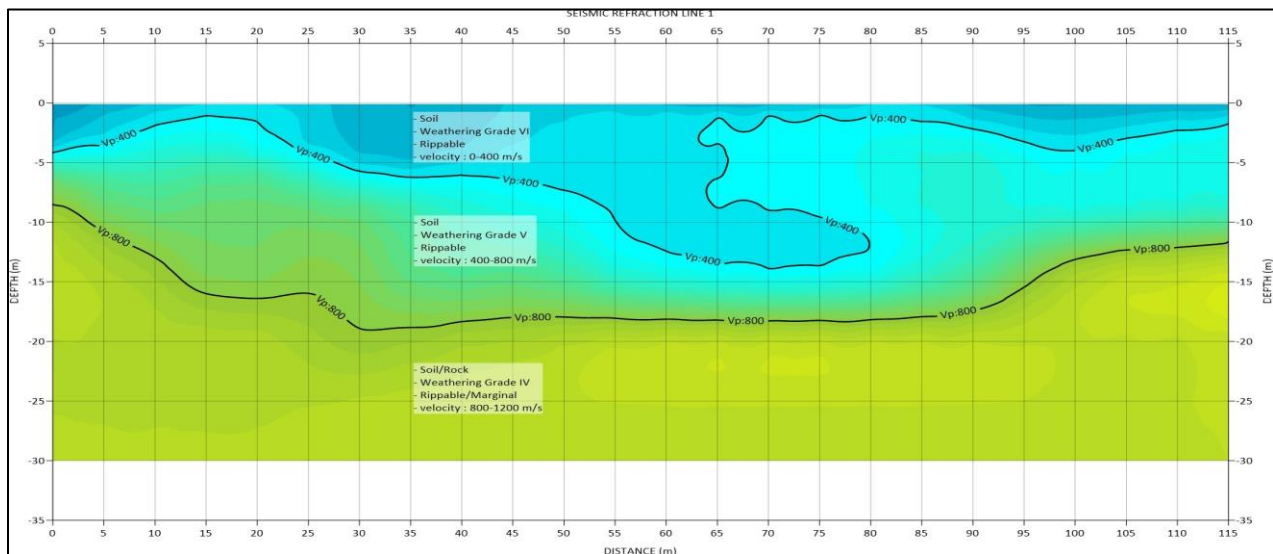


Fig. 14 Profile seismic line

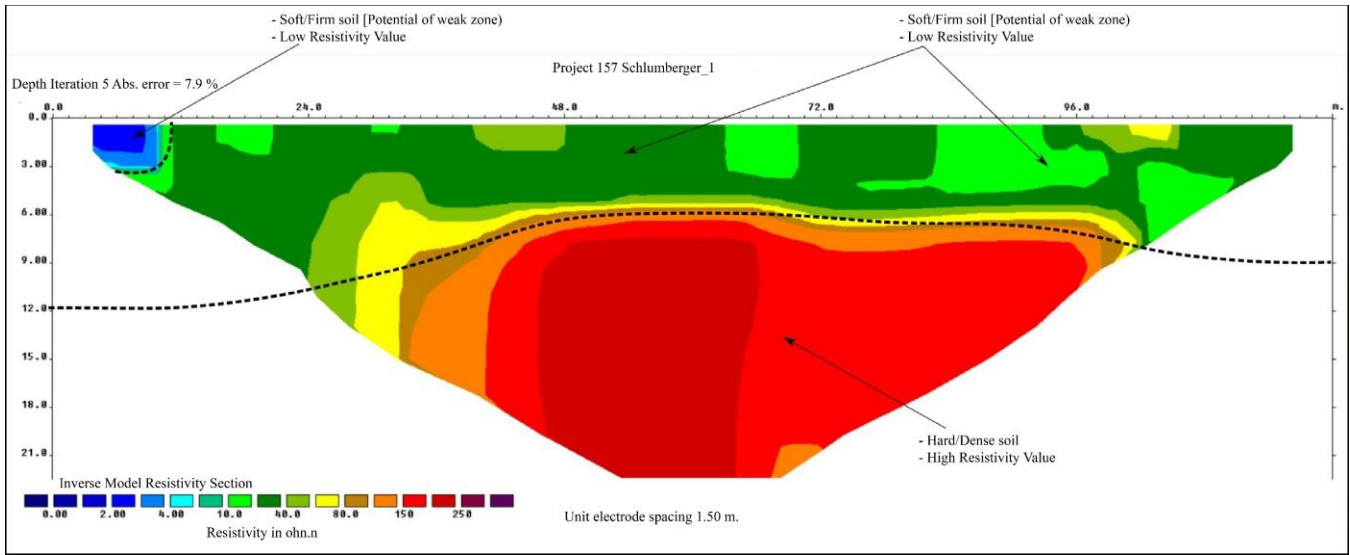


Fig. 15 Profile resistivity line (protocol schlumberger)

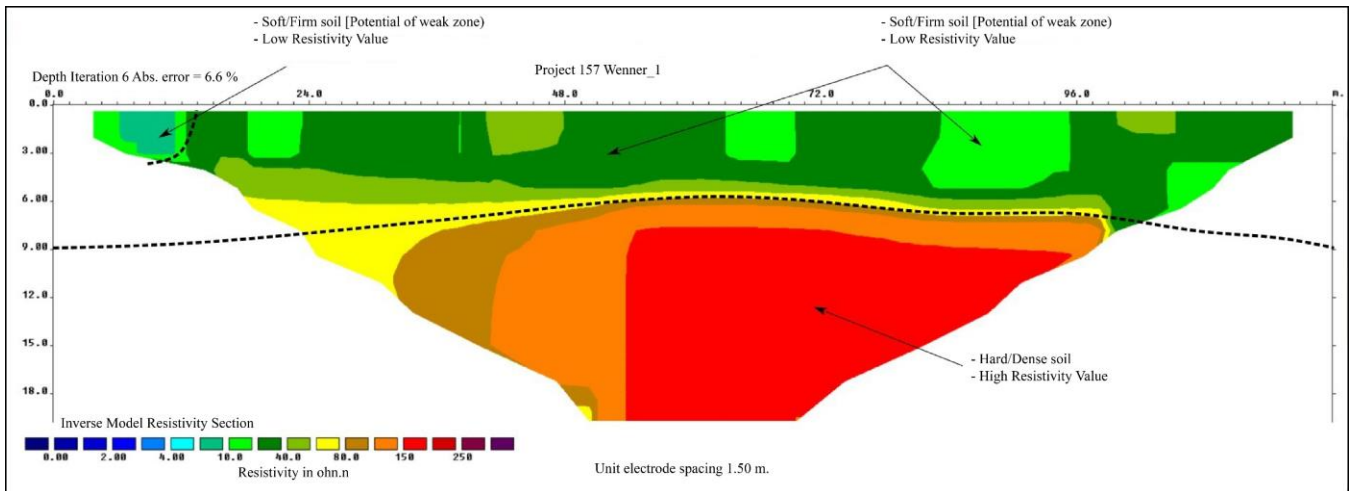


Fig. 16 Profile resistivity line (protocol wenner)

### 6.2.2. Results of ERI Line (PROTOCOL WENNER)

As can be observed from Figure 16, Similar to the observations with approximately showing similar ohm.m values from *PROTOCOL SCHLUMBERGER*, the ERI results for *PROTOCOL WENNER* also identify a top layer extending to a depth of approximately 6-9 meters, interpreted as potential fill material that likely remains uncompacted. Beneath this layer, another dense anomaly is presumed to be either compacted soil or the original layer. In this case, bedrock is also not clearly discernible in this ERI profile, indicating that it is likely deeper than the surveyed depth.

## 7. Conclusion

This study utilized two geophysical survey methods- seismic refraction and Electrical Resistivity Imaging (ERI)- to characterize subsurface layers. The ERI data was analyzed using two protocols: Schlumberger and Wenner. Through these analyses, three distinct subsurface layers were

identified. Results from both ERI and seismic refraction surveys consistently characterized the uppermost soil layer as potential fill material, likely consisting of loosely compacted soil, reaching depths of 6-9 meters and classified as Weathering Grade VI, indicating material that is completely rippable or fills. Beneath this layer, both methods detected an anomaly indicating a denser, possibly compacted or naturally deposited soil layer, classified as Weathering Grade V. A third layer was identified beyond 15 meters, representing soil with a Weathering Grade IV classification, which may be marginally rippable. Neither ERI nor seismic refraction methods detected bedrock within the surveyed depth, suggesting it lies deeper than the range of these methods.

The combined use of seismic refraction and Electrical Resistivity Imaging provided effective results for assessing layer thickness without disturbing the soil. This integrated approach demonstrated that using multiple methods yields

more reliable and precise interpretations of subsurface conditions, enhancing data accuracy. These findings significantly improve our understanding of soil structure to the surveyed depth and underscore the limitations of these methods in detecting deeper bedrock, which may require alternative geophysical techniques or deeper drilling for confirmation.

Furthermore, the interpretations derived from this study offer valuable insights for subsequent stages of site investigation, including risk assessment, soil stability analysis, and foundation planning. The results can guide decisions about suitable foundation types and depths, selecting construction materials, and designing stabilization measures, ultimately contributing to more resilient infrastructure. Overall, the study exemplifies how integrating geophysical survey methods can improve the accuracy of site characterization and enhance the sustainability and cost-effectiveness of engineering projects.

The field evaluation and geophysical analyses in this study were conducted in accordance with current practices, acknowledging the inherent advantages and limitations of each method. While the combination of seismic refraction and electrical resistivity imaging provided valuable insights into subsurface conditions, no geophysical survey is

exhaustive, and some uncertainties remain. The interpretations presented in this study are based on available data and may not capture all variations in subsurface conditions. To improve accuracy and reduce uncertainties, further subsurface exploration, such as borehole drilling along each survey line, is recommended to validate and refine the geophysical findings. Additionally, future research could incorporate 3D resistivity surveys to enhance the precision of subsurface characterization and provide a more comprehensive understanding of soil and rock distribution. These advancements would further strengthen site investigation methodologies and contribute to more reliable engineering and construction practices.

### Funding Statement

This research paper and all related research activities were funded by MAHSA University.

### Acknowledgement

The authors are thankful to the MIRO BUMI ENGINEERING team, as well as the staff and students from the Faculty of Engineering, Built Environment, and IT at MAHSA University, for their contributions to data acquisition. Their valuable insights and feedback also played a crucial role in refining the writing and presentation of this work.

### References

- [1] *Geotechnical Site Investigations for Underground Projects*, National Academy Press, pp. 1-423, 1984. [[Google Scholar](#)] [[Publisher Link](#)]
- [2] G.S. Littlejohn, K. Cole, and T.W. Mellors, "Without Site Investigation Ground is a Hazard," *Proceedings of the Institution of Civil Engineers, Civil Engineering*, vol. 102, no. 2, pp. 72-78, 1994. [[CrossRef](#)] [[Google Scholar](#)] [[Publisher Link](#)]
- [3] Raymond L. Nordlund, and Don U. Deere, "Collapse of Fargo Grain Elevator," *Journal of Soil Mechanics and Foundations Division*, vol. 96, no. 2, pp. 585-607, 1970. [[CrossRef](#)] [[Google Scholar](#)] [[Publisher Link](#)]
- [4] Magdi Zumrawi, "Effects of Inadequate Geotechnical Investigation on Civil Engineering Projects," *International Journal of Science and Research*, vol. 3, no. 6, pp. 927-931, 2014. [[Google Scholar](#)] [[Publisher Link](#)]
- [5] Mark Jaksa, "Geotechnical Risk and Inadequate Site Investigations: A Case Study," *Australian Geomechanics*, vol. 35, no. 2, pp. 39-46, 2000. [[Google Scholar](#)]
- [6] John Connaughton, and Lawrence Mbugua, "*Faster Building for Industry: NEDO (1983)*," *Construction Reports 1944-98*, 1983. [[CrossRef](#)] [[Google Scholar](#)] [[Publisher Link](#)]
- [7] P.M. Soupios et al., "Use of Engineering Geophysics to Investigate a Site for a Building Foundation," *Journal of Geophysics and Engineering*, vol. 4, no. 1, pp. 94-103, 2007. [[CrossRef](#)] [[Google Scholar](#)] [[Publisher Link](#)]
- [8] Kumari Sudha et al., "Soil Characterization Using Electrical Resistivity Tomography and Geotechnical Investigations," *Journal of Applied Geophysics*, vol. 67, no. 1, pp. 74-79, 2009. [[CrossRef](#)] [[Google Scholar](#)] [[Publisher Link](#)]
- [9] O.J. Akintorinwa, and O. Abiola, "Subsoil Evaluation for Pre-Foundation Study using Geophysical and Geotechnical Approach," *Journal of Emerging Trends in Engineering and Applied Sciences*, vol. 2, no. 5, pp. 858-863, 2011. [[Google Scholar](#)] [[Publisher Link](#)]
- [10] E.T. Faleye, and G.O. Omosuyi, "Geophysical and Geotechnical Characterisation of Foundation Beds at Kuchiyaku, Kuje Area, Abuja, Nigeria," *Journal of Emerging Trends in Engineering and Applied Sciences*, vol. 2, no. 5, pp. 864-870, 2011. [[Google Scholar](#)] [[Publisher Link](#)]
- [11] Esam Ismail et al., "Applying Geophysical and Hydrogeochemical Methods to Evaluate Groundwater Potential and Quality in Middle Egypt," *Hydrology*, vol. 10, no. 8, pp. 1-18, 2023. [[CrossRef](#)] [[Google Scholar](#)] [[Publisher Link](#)]
- [12] Ayuni Ngo Kilian et al., "Geo-Electrical Investigation of Groundwater for Hand Pump Borehole at Garin Mallum Ardo Kola Local Government Area, Taraba State, Ne Nigeria," *International Journal of Technical Research & Science*, vol. 3, no. 8, pp. 276-281, 2018. [[CrossRef](#)] [[Google Scholar](#)] [[Publisher Link](#)]

- [13] M.S.I. Zaini et al., "Granite Exploration by Using Electrical Resistivity Imaging (ERI): A Case Study in Johor," *International Journal of Integrated Engineering*, vol. 12, no. 8, pp. 328-347, 2020. [[CrossRef](#)] [[Google Scholar](#)] [[Publisher Link](#)]
- [14] S.K. Maniruzzaman, "Identification of Groundwater in Hard Rock Terrain using 2D Electrical Resistivity Tomography Imaging Technique: Securing Water Scarcity at the Time of Seasonal Rainfall Failure, South Andaman," *International Journal of Geosciences*, vol. 9, no. 1, pp. 59-70, 2018. [[CrossRef](#)] [[Google Scholar](#)] [[Publisher Link](#)]
- [15] Z.A.M. Hazreek "Soil Identification Using Field Electrical Resistivity Method," *Journal of Physics Conference Series*, vol. 622, pp. 1-7. 2015. [[CrossRef](#)] [[Google Scholar](#)] [[Publisher Link](#)]
- [16] O.C.B. Gandolfo, G. Mondelli, and R.G. Blanco, "The Use of Geophysical Methods to Investigate a Contaminated Site with Organochlorine," *Geotechnical and Geophysical Site Characterization: Proceedings of the 4<sup>th</sup> International Conference on Site Characterization ISC-4*, Boca Raton, vol. 1, pp. 1375-1380, 2013. [[Google Scholar](#)]
- [17] Olawale Olakunle Osinowo, and Michael Oluseyi Falufosi, "3D Electrical Resistivity Imaging (ERI) for Subsurface Evaluation in Pre-Engineering Construction Site Investigation," *NRIAG Journal of Astronomy and Geophysics*, vol. 7, no. 2, pp. 309-317, 2018. [[CrossRef](#)] [[Google Scholar](#)] [[Publisher Link](#)]
- [18] Hermann J. Mauritsch, "Geophysical Investigations of Large Landslides in the Carnic Region of Southern Austria," *Engineering Geology*, vol. 56, no. 3-4, pp. 373-388, 2000. [[CrossRef](#)] [[Google Scholar](#)] [[Publisher Link](#)]
- [19] Rhett Herman, "An Introduction to Electrical Resistivity in Geophysics," *American Journal of Physics*, vol. 69, pp. 943-952, 2001. [[CrossRef](#)] [[Google Scholar](#)] [[Publisher Link](#)]
- [20] D.J. Gobbett, and C.S. Hutchinson, *Geology of the Malay Peninsula (West Malaysia and Singapore)*, Geological Magazine, vol. 111, no. 2, pp. 183-183, 1974. [[CrossRef](#)] [[Google Scholar](#)] [[Publisher Link](#)]
- [21] Charles Strachan Hutchison, and Cedric Keith Burton, *Geology of the Malay Peninsula: (West Malaysia and Singapore)*, Wiley-Interscience, pp. 1-438, 1973. [[Google Scholar](#)] [[Publisher Link](#)]
- [22] Xianhuai Zhu, and George A. McMechan, "Estimation of Two-Dimensional Seismic Compressional Wave Velocity Distribution by Interactive Tomographic Imaging," *International Journal of Image System and Technology*, vol. 1, no. 1, pp. 13-17, 1989. [[CrossRef](#)] [[Google Scholar](#)] [[Publisher Link](#)]
- [23] Joseph P. Stefani, "Turning-Ray Tomography," *Geophysics*, vol. 60, no. 6, pp. 1971-1929, 1995. [[CrossRef](#)] [[Google Scholar](#)] [[Publisher Link](#)]
- [24] I.N. Azwin, Rosli Saad, and M. Nordiana, "Applying the Seismic Refraction Tomography for Site Characterization," *APCBEE Procedia*, vol. 5, pp. 227-231, 2013. [[CrossRef](#)] [[Google Scholar](#)] [[Publisher Link](#)]
- [25] F.P. Haeni, "Application of Continuous Seismic Reflection Methods to Hydrologic Studies," *Groundwater*, vol. 24, no. 1, pp. 23-31, 1986. [[CrossRef](#)] [[Google Scholar](#)] [[Publisher Link](#)]
- [26] Umar Hamzah, and Abd Rahim Samsudin, "2D Seismic Refraction Tomography Survey on Metasedimentary at a Proposed Development Site in Dengkil, Selangor," *Bulletin of the Geological Society of Malaysia*, no. 52, pp. 1-6, 2006. [[CrossRef](#)] [[Google Scholar](#)] [[Publisher Link](#)]
- [27] Mohd Rozi Umor et al., "Determination Layer of Meta-Sediment Rock Using Seismic Refraction Survey at the Vicinity of Alor Gajah Town, Melaka, Peninsular Malaysia," *International Journal of Advanced and Applied Sciences*, vol. 3, no. 5, pp. 65-72, 2016. [[Google Scholar](#)] [[Publisher Link](#)]
- [28] Sulaiman Mohd, and Abioga Mahendra, "Application of Electrical Resistivity Imaging (ERI) to Analyse Geological Structure in Paloh, Gua Musang, Kelantan," *BIO Web of Conferences*, vol. 73, pp. 1-6, 2023. [[CrossRef](#)] [[Google Scholar](#)] [[Publisher Link](#)]
- [29] George Vernon Keller, and Frank C. Frischknecht, *Electrical Methods in Geophysical Prospecting*, Pergamon Press, pp. 1-523, 1966. [[Google Scholar](#)] [[Publisher Link](#)]
- [30] W. Wightman, *Application of Geophysical Methods to Highway Related Problems*, Federal Highway Administration, Office of Bridge Technology, pp. 1-716, 2004. [[Google Scholar](#)] [[Publisher Link](#)]
- [31] Jamaluddin, and Emi Prasetyawati Umar, "Identification of Subsurface Layer with Wenner-Schlumberger Arrays Configuration Geoelectrical Method," *IOP Conference Series: Earth and Environmental Science*, vol. 18, pp. 1-6, 2017. [[CrossRef](#)] [[Google Scholar](#)] [[Publisher Link](#)]
- [32] R.P. Martin, and S.R. Hencher, "Principles for Description and Classification of Weathered Rock for Engineering Purposes," *Geological Society, London, Engineering Geology Special Publications*, vol. 2, pp. 299-308, 1986. [[CrossRef](#)] [[Google Scholar](#)] [[Publisher Link](#)]
- [33] M.A.M. Ismail et al., "Rippability Assessment of Weathered Sedimentary Rock Mass Using Seismic Refraction Methods," *Journal of Physics: Conference Series*, vol. 995, pp. 1-9, 2018. [[CrossRef](#)] [[Google Scholar](#)] [[Publisher Link](#)]
- [34] *Handbook of Ripping*, 12<sup>th</sup> ed., Caterpillar, Peoria, Illinois, pp. 1-32, 2000. [[Publisher Link](#)]
- [35] W.M. Telford, L.P. Geldart, and R.E. Sheriff, *Resistivity Methods, Applied Geophysics*, Cambridge University Press, pp. 522-577, 1990. [[CrossRef](#)] [[Google Scholar](#)] [[Publisher Link](#)]
- [36] G.J. Palacky, *Resistivity Characteristics of Geologic Targets*, Electromagnetic Methods in Applied Geophysics, vol. 1, 1987. [[CrossRef](#)] [[Google Scholar](#)] [[Publisher Link](#)]